


# High-efficiency switchable optical elements for advanced head-up displays

Tao Zhan SID Student Member<sup>1</sup> | Yun-Han Lee SID Student Member<sup>1</sup> |

Jianghao Xiong SID Student Member<sup>1</sup> | Guanjun Tan SID Student Member<sup>1</sup> |

Kun Yin SID Student Member<sup>1</sup> | Jilin Yang<sup>2</sup> | Sheng Liu<sup>2</sup> | Shin-Tson Wu SID Fellow<sup>1</sup> 

<sup>1</sup>College of Optics and Photonics,  
University of Central Florida, Orlando,  
Florida

<sup>2</sup>GoerTek Electronics, 5451 Great  
America Parkway, Suite 301, Santa Clara,  
California

## Correspondence

Shin-Tson Wu, College of Optics and  
Photonics, University of Central Florida,  
Orlando, FL 32816.

Email: swu@ucf.edu

## Funding information

GoerTek Electronics; Intel Corporation;  
GoerTek; Intel

## Abstract

The Pancharatnam-Berry optical elements (PBOEs) are utilized to enhance the performance of head-up displays (HUDs). The Pancharatnam-Berry lenses (PBLs) provide varifocal functionality and compensate chromatic aberrations, while the Pancharatnam-Berry deflectors (PBDs) can function as optical combiners and waveguide couplers. Moreover, the Rigorous coupled wave analysis (RCWA) based on the scattering matrix is developed and applied in the structure optimization of PBOEs for HUD applications.

## KEYWORDS

adaptive optics, head-up display, liquid crystal device, Pancharatnam-Berry phase

## 1 | INTRODUCTION

With the rapid development of high brightness yet compact display systems and increasing needs from the modern automobile industry, head-up displays (HUDs), aimed at enhancing road safety and driving comfort, have been intensively developed in recent years.<sup>1–3</sup> The very name “head-up” precisely and concisely emphasizes the main benefit of this type of automotive display. Useful driving information such as navigation instructions, adaptive cruise control data, and lane-departure warnings are directly projected to the driver's field of view (FOV). The driver could conveniently process the necessary graphics displayed in front of the windshield, holding his/her attention on the traffic without shifting or refocusing of eyesight, just like a pilot of a jet fighter.

Although HUDs have already been installed in some commercial vehicles, several critical technical issues remain to be addressed. So far, most commercialized HUDs project the virtual image at a fixed distance, typically around 2.5 m in front of the driver. However, the driver may not focus on the fixed virtual image distance

(VID) in different driving circumstances, such as driving fast on highways and relatively slow in local lanes. The display brightness and total power efficiency is another big concern in HUDs. For the driver to perceive the image contents, a tolerable ambient contrast ratio, say  $>3:1$ , has to be maintained under various ambient conditions, which is quite challenging especially when the sunlight is strong. Such a brightness issue may become more severe in next-generation HUDs with an enlarged FOV and longer VID.

In this paper, we propose to integrate the Pancharatnam-Berry optics elements (PBOEs)<sup>4–6</sup> into next-generation HUD systems to deal with the issues above-mentioned. Firstly, the working principle and the functionalities of PBOEs are introduced. After that, the application of PBOEs in HUDs are demonstrated in details. The VID could be adaptively changed in less than one millisecond with switchable PBLs for various driving environments. Simultaneously, the look down angle (LDA) could also be switched accordingly by PBDs to keep the virtual image on the road. Moreover, the reflective Bragg PBD<sup>7–9</sup> is a promising candidate as a polarization-selective high-efficiency optical combiner (OC) for higher total power efficiency and thus better contrast

ratio. In the emerging waveguide-type HUDs, the reflective Bragg PBDs could double the FOV and significantly reduce the component volume. We also developed a rigorous coupled wave analysis (RCWA)<sup>10</sup> simulation method to optimize the spectral and angular performance of PBOE structures for various HUD applications.

## 2 | OPERATION PRINCIPLE

Liquid crystal Pancharatnam-Berry optical elements are essentially functional planar structures with a spatial-varying anisotropy. By changing the anisotropy distribution, arbitrary phase pattern could be achieved in theory, including but not limited to the deflector, lens and even microlens arrays. Thanks to their approximately 100% diffraction efficiency, strong polarization selectivity, and low fabrication cost, PBOEs could be well utilized in various kinds of emerging display applications<sup>11,12</sup> for performance enhancement.

The PBOEs in the Raman-Nath regime can be understood as a patterned half-wave plate with in-plane variation in crystal axis, denoted as  $\Psi(x,y)$ . With a circularly polarized input light, Jones calculus can be established as follows:

$$J_{out} = R(-\psi)W(\pi)R(\psi)J_{in} = -je^{\pm 2j\psi}J_{\mp}, \quad (1)$$

$$J_{in} = J_{\pm} = \frac{1}{\sqrt{2}} \begin{bmatrix} 1 \\ \pm j \end{bmatrix}, \quad (2)$$

where  $R(\Psi)$  is the rotation matrix,  $W(\pi)$  is the retardation Jones matrix of half-wave plate, and  $J_{\pm}$  is the Jones vector of right-handed circular polarized (RCP) and left-handed circular polarized light (LCP). It is observed that the spatial-varying phase pattern could be arbitrarily generated by patterning the azimuthal angle of liquid crystal orientation. Based on this concept, PBOEs with lens<sup>13,14</sup> and grating<sup>15,16</sup> patterns are depicted in Figure 1A. It should be emphasized that the phase accumulation of PBOEs manifest opposite signs for RCP and LCP. As a result, a PBL may function as a converging lens for RCP input but a diverging one for LCP, as shown in Figure 1B. Similarly, a PBD would diffract RCP and LCP into opposite directions.

With their distinct polarization dependency and electro-optic response of liquid crystals, two types of dynamic switching can be realized: active and passive. For passive switching, the PBOEs are made of liquid crystal polymers, which are not switched directly. Instead, we place an electrically switchable polarization rotator (eg, a 90° twist-nematic [TN] LC cell with a  $\lambda/4$  plate) in front of the PBOE. By controlling the polarization handedness of the incoming beam, the PBOE will function differently. For active switching, the PBOEs are usually made of liquid crystal cells using indium tin oxide (ITO) glass substrates. By directly applying a voltage across the PBOE device, the LC directors will be reoriented from the patterned half-wave plate to homeotropic state, and the optical function of PBOEs vanishes immediately. Table 1

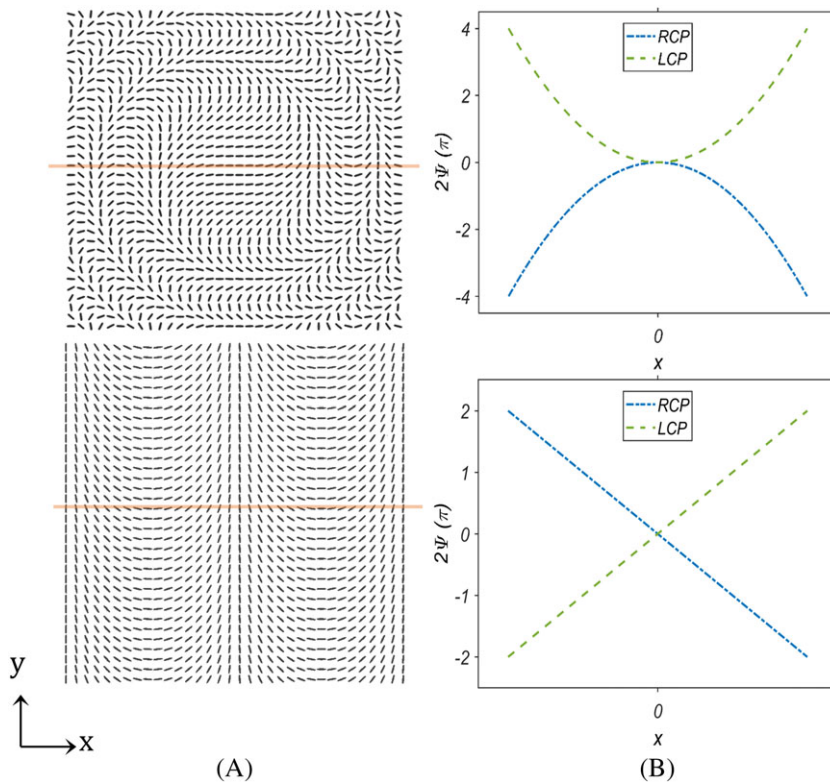


**FIGURE 1** A, The schematic illustration of liquid crystal anisotropy axis orientation in Raman-Nath Pancharatnam-Berry optical elements (PBOEs) and B, according spatial phase change for orthogonal circular polarizations

**TABLE 1** Electric and polarization response of PBOEs in the Raman-Nath regime

Input polarization	W/o Voltage		W/voltage
	RCP	LCP	NA
PBL optical power	K	-K	0
PBD diffraction order	1	-1	0
Output polarization	LCP	RCP	NA

Abbreviation: LCP, left-handed circular polarizer; PBOEs, Pancharatnam-Berry optical elements; RCP, right-handed circular polarizer.

summarizes the driving schemes of PBDs and PBLs with their corresponding optical effects.

PBOEs in Bragg regime, usually with a higher degree of twist in the axial ( $z$  axis) direction than those in Raman-Nath regime, could be fabricated by adding some chiral dopants into the host LC mixture, whose anisotropy axis orientation patterns are illustrated in Figure 2. The Bragg PBOEs could be made either transmissive or reflective by engineering their twist structures. With numerous periods in the axial direction, Bragg PBOEs generally provide a larger deflection angle and manifest higher spectral and angular selectivity than the PBOEs in Raman-Nath regime, which enables useful HUD applications such as narrowband polarization-selective OCs and waveguide-display grating couplers.

### 3 | APPLICATIONS TO HUDS

#### 3.1 | Switchable VIDs and look-down angles

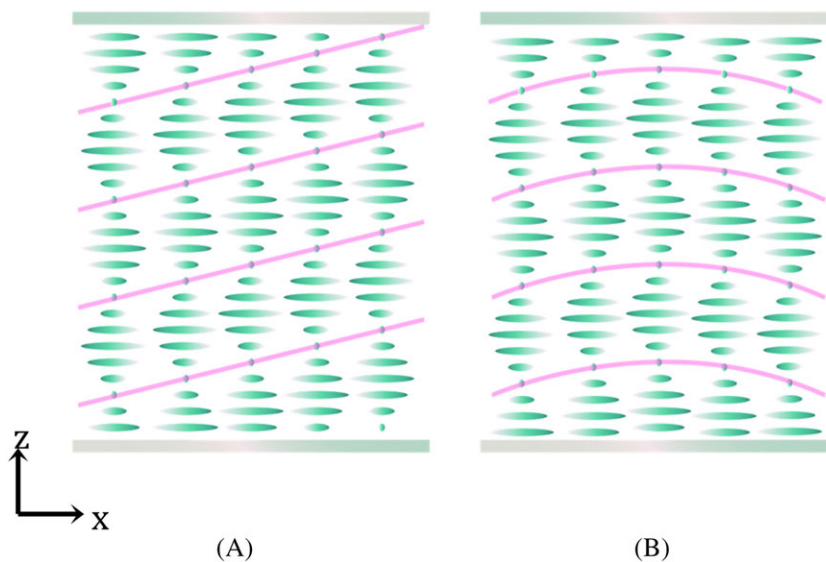
Figure 3 illustrates the optical setup of a conventional projection-type HUD for automobile displays. The image

from the display panel (DP) is projected toward the windshield by the curved mirrors (M1 and M2). The optical power of the mirrors determines the VID. A transmissive PBL (or PBD) is placed between the curved mirror system and the OC to control the virtual image distance (or look down angle). Utilizing the polarization selective nature of polymeric PBLs, the virtual image depth can be switched by simply changing the input polarization states to accommodate different driving circumstances.

Before integrating PBLs into HUD system, the polarization-dependent focal length of PBLs is verified from the apparatus illustrated in Figure 4A. The left and right side of the display light is converted to LCP and RCP by a pair of circular polarizers. The virtual image content is then observed through a PBL, as Figure 4B shows. Because of the PBL, the image is separately displayed at different distances by controlling the polarization state of incoming light at a different part of FOV. With a patterned circular polarizer integrated into the conventional HUD system, as depicted in Figure 3, the HUD image can be directly displayed at two image distances. Furthermore, with a polarization converter (usually made of fast-response twisted-nematic LC) placed before the PBL, the VID can be conveniently switched. To prove the concept, in Figure 5, a PBL is integrated into a simplified HUD system, where a doublet lens replaces the curved mirrors. Moreover, a multiplane light field HUD is also applicable through time<sup>17</sup> or polarization<sup>18</sup> multiplexing.

Similarly, PBDs can also be employed as image shifter<sup>19</sup> to adaptively change the look-down angle through the same operation approaches for PBLs as mentioned above. With PBDs placed in the projection system, the whole virtual image or even part of it could be shifted to different angles for various driving circumstances.

**FIGURE 2** The schematic illustration of liquid crystal anisotropy axis orientation in reflective A, Pancharatnam-Berry deflectors (PBD) and B, Pancharatnam-Berry lenses (PBL)



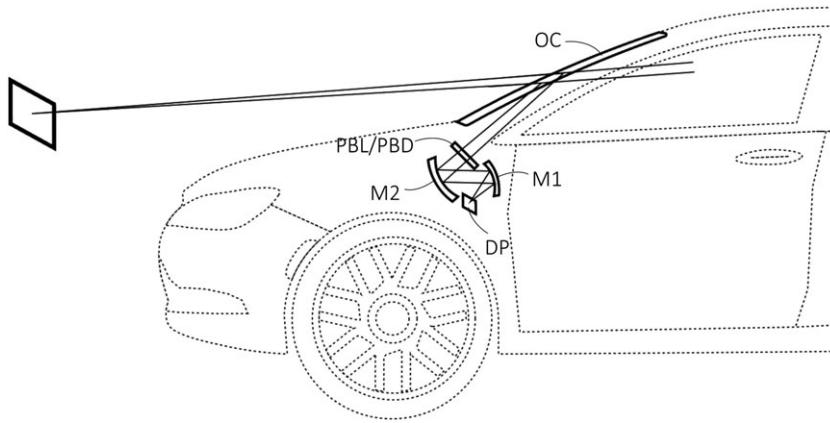


**FIGURE 3** Schematics of the optics in a direct projection type HUD, where DP: display panel; M: mirror; OC: optical combiner (windshield)

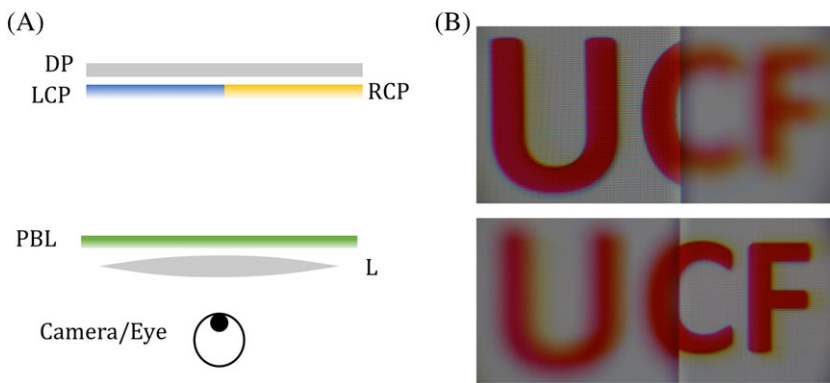


**FIGURE 4** A, Experiment setup and B, photographs of two virtual image distances (VID) enabled by polarization selective focal length of a Pancharathnam-Berry lenses (PBL) (DP: display panel; LCP: left-handed circular polarizer; RCP: right-handed circular polarizer; L: refractive lens)

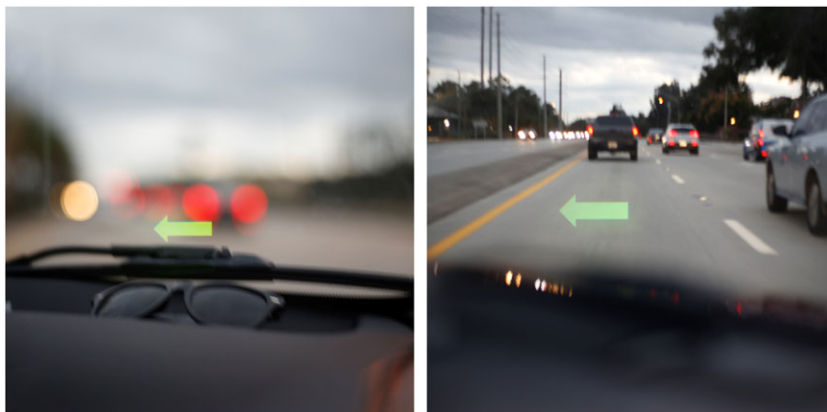


**FIGURE 5** Photograph captured through a head-up displays (HUD) focusing at (left) short and (right) long virtual image distance enabled by a passive-driven Pancharathnam-Berry lenses (PBL)

Moreover, with PBDs continuously switching on and off, the FOV of HUD systems can be effectively enlarged if a fast-response display engine is available.

### 3.2 | Polarization-sensitive see-through OC

In the HUDs developed for automobile and aviation industries, high-quality OCs are vital components to combine the projected graphics and the see-through external environment. While most aftermarket HUDs are equipped

with an independent OC, HUDs from original equipment manufacturers (OEM) usually directly employ the windshield as a simple OC for better see-through quality and smaller form factor. Because of the enforced requirement of high transmittance for the safety of drivers, the allowed windshield reflectivity is highly limited, typically less than 25%, resulting in a significant loss of the light from the optical engine. Thus, relatively narrowband combiners that share similar functional spectrum range to display light from the HUD light engine can be applied to increase the optical efficiency, while maintaining the required transmittance. Since the reflective PBOEs are mainly in



the Bragg regime, they usually manifest high-diffraction efficiency in a narrow spectral band in comparison with the transmissive PBOEs. And the functional band of reflective PBOEs could be easily tuned by using polymerizable LCs with different birefringence, similar to a thick cholesteric liquid crystal layer. For example, the first-order diffraction efficiency of a reflective PBD with 678-nm grating period and 182-nm helix twist pitch is simulated, and the results are plotted in Figure 6. For a fixed incident angle, the location of the reflection band can be easily tuned to RGB wavelengths by changing the helix twist pitch of reflective PBOEs while using the same LC polymer. It is also applicable to cascade polymeric PBDs with different reflection bands to achieve deflection at RGB wavelengths for a full-color HUD. Moreover, to maintain high-efficiency with an increased incident angle, a

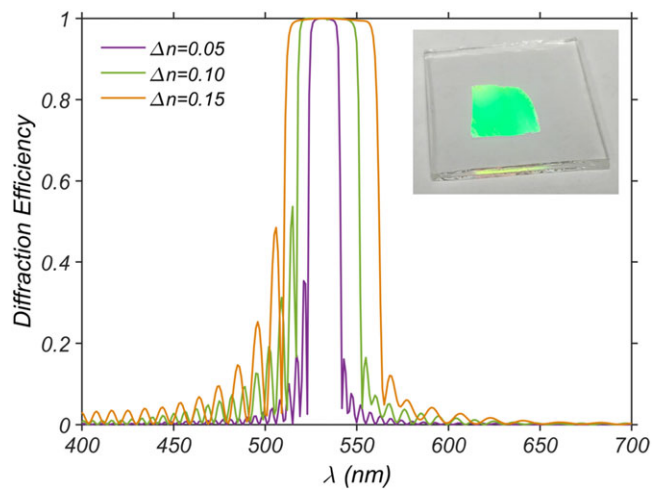


**FIGURE 6** Simulated spectral response of reflective Pancharatnam-Berry deflectors (PBDs) made of liquid crystal polymers with different birefringence

gradient pitch method can be applied to fabricate chirped PBDs, which was originally designed for cholesteric liquid crystals. The diffraction efficiency of reflective Bragg PBDs could be conveniently tailored as well, from 0% to 100%, through controlling the thickness of the LC polymer layer. Also, because a single-layer reflective PBOE deflects one handedness of light polarization and transmits the other, more margin is achieved when evaluating the trade-off between transmittance and reflectance of the OC with unpolarized environmental light and a polarized display light. As a result, with the same apparent transparency, the ambient contrast ratio is considerably enhanced compared with the conventional half-mirror approach.

Moreover, the PBOE made of liquid crystal polymer can be fabricated on a flexible substrate and then laminated onto a curved surface. Thus, similar to holographic optical elements (HOEs), it is applicable to laminate reflective PBOEs with customized phase patterns on curved surfaces, including the windshield in OEM HUDs and also the combiner screen in aftermarket ones.

### 3.3 | Coupler for waveguide-type HUD

HUDs based on the waveguide structure<sup>20</sup> have been developed because of their enlarged FOV and compact form factor. Although this kind of structure behaves more like a lightguide, it is commonly referred to as “waveguide” display. The input and output grating couplers are essential optical components in the waveguide displays.<sup>21</sup> The input PBD attached to one side of the waveguide accepts the incident beam from the display engine and deflects it into the waveguide. To satisfy the condition of total internal reflection, the grating period is customized according to the refractive index of the waveguide and

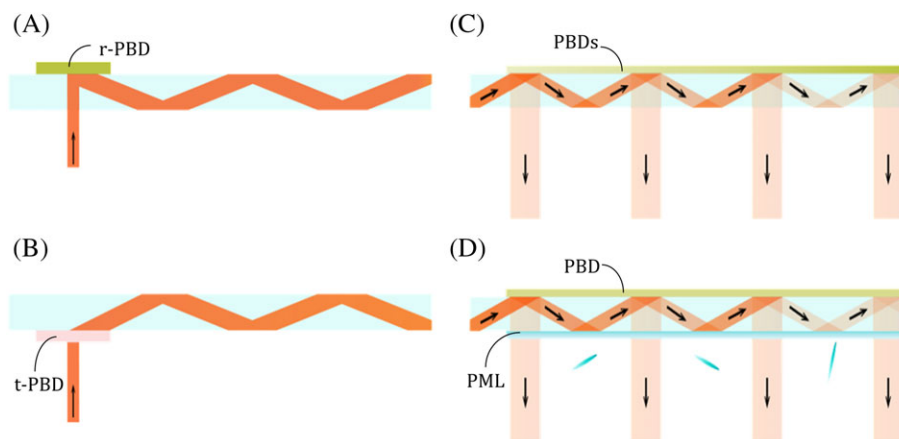


**FIGURE 7** Side view of waveguide HUD input couplers employing A, reflective Pancharatnam-Berry deflectors (r-PBD), B, transmissive Pancharatnam-Berry deflectors (t-PBD) and output pupil expansion using C, efficiency-varying output grating couplers and D, a uniform-efficiency output grating coupler with a polarization management layer (PML)

LC polymer. The input coupler should manifest high efficiency for the first-order diffraction within an acceptable FOV. Higher-order diffractions should be minimized for efficient light utilization and reduced stray light. Both transmissive (t-PBD) and reflective (r-PBD) Bragg PBDs can be made by tuning helix twist pitch of the LC structure, which is usually controlled by the concentration of chiral dopants. And both of them are applicable as input grating couplers, as Figure 7A,B depict. Although both r-PBD and t-PBD can provide greater than 95% diffraction efficiency for a circularly polarized light, the diffraction efficiency of r-PBDs increases as the LC polymer gets thicker,<sup>22</sup> while that of t-PBD shows a more sophisticated dependence on the thickness.<sup>23</sup> Consequently, the thickness control of high-efficiency t-PBDs is more stringent than that of r-PBDs.

When the light is extracted from the waveguide through an output grating coupler, an exit-pupil-replication method is usually applied to enlarge the usable eye box. Since light intensity decreases each time it encounters the output coupler, an output coupler with spatial-varying diffraction efficiency is commonly employed to ensure a relatively uniform output intensity from each replicated exit pupil. This approach should be applied more cautiously when the VID is very short, since the output image may appear at several different VIDs because of different propagation length in the waveguide. Generally, each successive out-coupling needs to be more efficient because of the intensity loss when the light propagates in such a leaky waveguide. Conventionally, the out-coupling efficiency is tuned by changing the structure of the grating itself, as illustrated in Figure 7C. By changing the thickness of the LC layer, spatial-varying diffraction efficiency can be achieved for PBDs. Considering the characteristic polarization dependency of PBDs, the out-coupling efficiency can also be controlled by the polarization of the

propagating light, utilizing a polarization management layer (PML),<sup>24</sup> as depicted in Figure 7D. The PML is a transparent anisotropic film with variable permittivity matrix along the waveguide, which controls the polarization state of display light and manifests no effects on the intensity of the see-through light. It is also worth mentioning that the polarization-based exit pupil replication method is suitable not only for PBD couplers but also for other grating couplers with high-polarization sensitivity. Thanks to the flat physical surface of PBDs, two-dimension exit pupil replication using PBDs can be conveniently achieved by not only the conventional spatial-separated cascading<sup>25</sup> but also crossed-overlapping<sup>26</sup> configuration, as illustrated in Figure 8A,B, respectively. And extra PMLs can be placed between the two PBDs to providing additional degrees of freedom for uniform out-coupling intensity, as depicted in Figure 9.

#### 4 | SIMULATION AND OPTIMIZATION BY RCWA

In order to simulate the diffraction efficiency of PBOEs for different wavelength and incident angles, a numerical simulation tool employing the RCWA is developed. The simulation is based on the scattering matrix formulation for efficient memory usage and convenient implementation. As shown in Figure 10, the diffraction efficiency of non-twist single-layer PBOEs is limited since the half-wave condition cannot be satisfied for the whole visible spectrum, while the fabrication process can be quite simple.<sup>27</sup> Also, the LC birefringence dispersion<sup>28</sup> described in Equation 3 deteriorate the situation:

$$\Delta n = G\lambda^2\lambda^{*2}/(\lambda^2 - \lambda^{*2}), \quad (3)$$

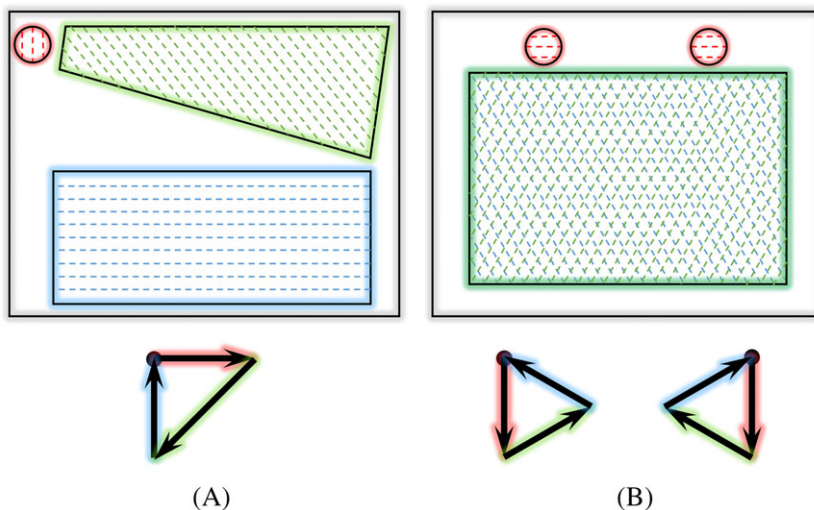


**FIGURE 8** Top view of coupler layout and according grating vectors in waveguide-type head-up displays (HUDs) employing A, an input grating, a turn grating, an output grating, and B, two or more independent input gratings with two crossed overlapping output gratings

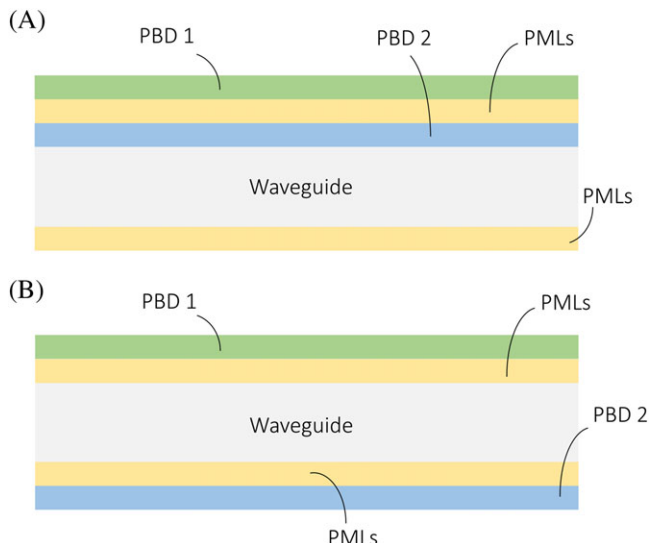


**FIGURE 9** Cross section of the two crossed overlapping output gratings with Pancharatnam-Berry deflectors (PBDs) on the A, same and B, both sides of the waveguide

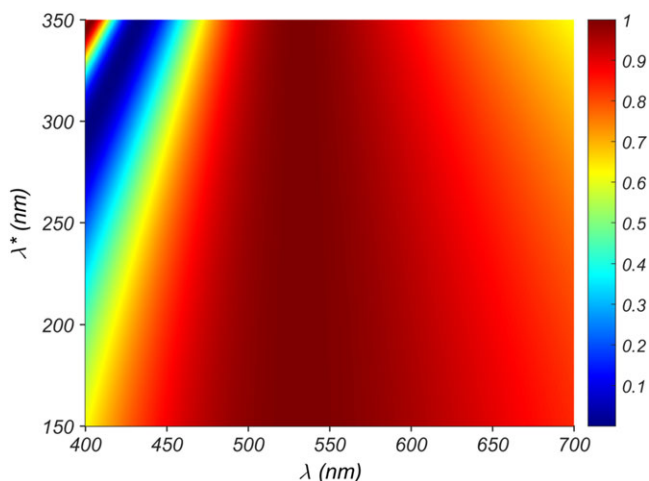


**FIGURE 10** Simulated first-order diffraction efficiency of Pancharatnam-Berry optical element (PBOE) in Raman-Nath regime employing liquid crystals with different birefringence dispersion

where  $G$  is the proportionality constant and  $\lambda^*$  is the mean resonance wavelength.

To achieve high-diffraction efficiency over a broader spectral range, especially at the three primary colors, a symmetrically twisted LC orientation in the axial direction<sup>16</sup> could be applied. Such a two-layer linear twist structure can effectively enlarge the high-efficiency bandwidth to cover most of the visible spectrum. Furthermore, by employing a nonlinear twist structure, such as polynomial or exponential, the broadband range of the symmetric two-layer structure can be even wider. Figure 11 shows a fitted birefringence of an LC reactive mesogen RM257 based on the data from Merck,<sup>29</sup> which is utilized

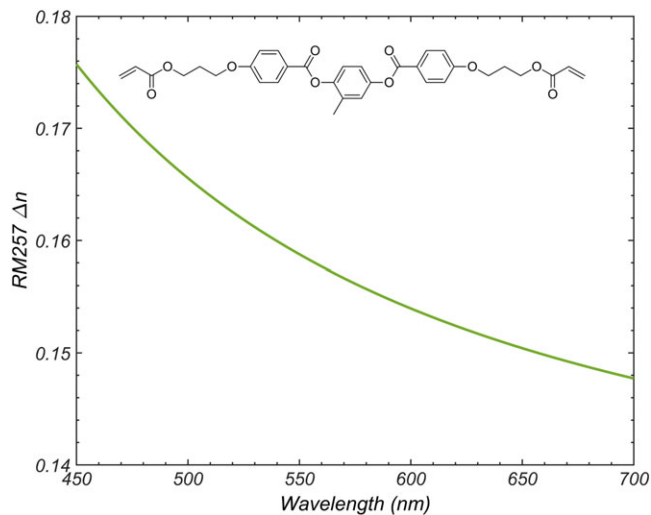


**FIGURE 11** Molecular structure and fitted birefringence dispersion of reactive mesogen RM257 in the visible spectrum, where  $G = 2.68 \mu\text{m}^{-2}$  and  $\lambda^* = 0.222 \mu\text{m}$  in Equation 3

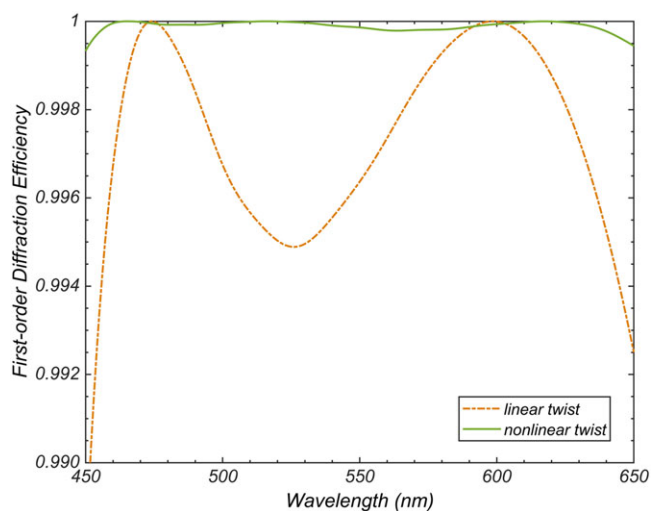


**FIGURE 12** Simulated first-order diffraction efficiency of Pancharatnam-Berry optical elements (PBOEs) with symmetric two-layer twist structures based on the birefringence of RM257

to compare the performance of linear and nonlinear twist structure. The LC orientation angle  $\psi$  in the first layer of the symmetric two-layer structures can be expressed as

$$\psi = \sum_{i=1}^n a_n \left(\frac{z}{d}\right)^n, z \in [0, d]. \quad (4)$$

And the second layer  $z \in [d, 2d]$  is symmetric to the first layer with respect to the plane  $z = d$ . Figure 12 depicts the first-order diffraction efficiency of two-layer structures with a linear ( $a_1 = 68.8^\circ$ ,  $d = 1.53 \mu\text{m}$ ) and nonlinear ( $a_1 = -6.75^\circ$ ,  $a_2 = -6.17^\circ$ ,  $a_3 = 112^\circ$ ,  $d = 2.28 \mu\text{m}$ ) twist. With more degrees of freedom, the

two-layer structure with a nonlinear twist can provide a broader bandwidth than that with a linear twist.

## 5 | CONCLUSION

The emerging PBOEs can boost the performance of HUDs in many perspectives. PBLs enable multiple or switchable virtual images distances for various driving circumstances. PBDs provide switchable looking down angle. The Bragg PBDs could function as a polarization-sensitive OC for better ambient contrast ratio and grating couplers for waveguide-type HUDs, significantly reducing the component volume while increasing the FOV.

## ACKNOWLEDGMENTS

The UCF group is indebted to Intel Corporation and GoerTek Electronics for the financial support.

## ORCID

Shin-Tson Wu  <https://orcid.org/0000-0002-0943-0440>

## REFERENCES

- Liu YC, Wen MH. Comparison of head-up display (HUD) vs. head-down display (HDD): driving performance of commercial vehicle operators in Taiwan. *Int J Human Computer Studies*. 2004;61(5):679–697. <https://doi.org/10.1016/j.ijhcs.2004.06.002>
- Hedili MK et al. Microlens array-based high-gain screen design for direct projection head-up displays. *Appl Optics*. 2013;52(6):1351–1357. <https://doi.org/10.1364/AO.52.001351>
- Cho WH et al. Head-up display using an inclined Al<sub>2</sub>O<sub>3</sub> column array. *Appl Optics*. 2014;53(4):A121–A124. <https://doi.org/10.1364/AO.53.00A121>
- Pancharatnam S. Generalized theory of interference and its applications. *Proc Indian Acad Sci, Sect a*. 1956;44(5):247–262. <https://doi.org/10.1007/BF03046050>
- Berry MV. Quantal phase factors accompanying adiabatic changes. *Proc R Soc London, Ser a*. 1984;392(1802):45–57. <https://doi.org/10.1098/rspa.1984.0023>
- Kim J et al. Fabrication of ideal geometric-phase holograms with arbitrary wavefronts. *Optica*. 2015;2(11):958–964. <https://doi.org/10.1364/OPTICA.2.000958>
- Kobashi et al. Planar optics with patterned chiral liquid crystals. *Nat Photonics*. 2016;10(6):389–392. <https://doi.org/10.1038/nphoton.2016.66>
- Weng et al. Polarization volume grating with high efficiency and large diffraction angle. *Opt Express*. 2016;24(16):17746–17759. <https://doi.org/10.1364/oe.24.017746>
- Chen R et al. Multi-stimuli-responsive self-organized liquid crystal Bragg gratings. *Adv Opt Mater*. 2019;7:1900101. <https://doi.org/10.1002/adom.201900101>
- Moharam MG et al. Formulation for stable and efficient implementation of the rigorous coupled-wave analysis of binary gratings. *J Opt Soc Am A*. 1995;12(5):1068–1076. <https://doi.org/10.1364/JOSAA.12.001068>
- Lee YH et al. Recent progress in Pancharatnam–Berry phase optical elements and the applications for virtual/augmented realities. *Optical Data Process Storage*. 2017;3(1):79–88. <https://doi.org/10.1515/odps-2017-0010>
- Zhan T et al. Pancharatnam–Berry optical elements for head-up and near-eye displays. *J Opt Soc Am B*. 2019;36(5):D52–D65. <https://doi.org/10.1364/JOSAB.36.000D52>
- Gao K et al. Thin-film Pancharatnam lens with low f-number and high quality. *Opt Express*. 2015;23(20):26086–26094. <https://doi.org/10.1364/OE.23.026086>
- Zhan T et al. Polarization-independent Pancharatnam–Berry phase lens system. *Opt Express*. 2018;26(26):35026–35033. <https://doi.org/10.1364/OE.26.035026>
- Gao K et al. High-efficiency large-angle Pancharatnam phase deflector based on dual-twist design. *Opt Express*. 2017;25(6):6283–6293. <https://doi.org/10.1364/OE.25.006283>
- Oh C, Escuti MJ. Achromatic diffraction from polarization gratings with high efficiency. *Opt Lett*. 2008;33(20):2287–2289. <https://doi.org/10.1364/OL.33.002287>
- Zhan T et al. High-resolution additive light field near-eye display by switchable Pancharatnam–Berry phase lenses. *Opt Express*. 2018;26(4):4863–4872. <https://doi.org/10.1364/OE.26.004863>
- Tan G et al. Polarization-multiplexed multiplane display. *Opt Lett*. 2018;43(22):5651–5654. <https://doi.org/10.1364/OL.43.005651>
- Tan G et al. Foveated imaging for near-eye displays. *Opt Express*. 2018;26(19):25076–25085. <https://doi.org/10.1364/OE.26.025076>
- Levola T, Aaltonen V. Near-to-eye display with diffractive exit pupil expander having chevron design. *J Soc Inf Display*. 2008;16(8):857–862. <https://doi.org/10.1889/1.2966447>
- Lee YH et al. Prospects and challenges in augmented reality displays. *Virtual Reality & Intelligence Hardware*. 2019;1(1):10–20. <https://doi.org/10.3724/SP.J.2096-5796.2018.0009>
- Lee YH et al. Reflective polarization volume gratings for high efficiency waveguide-coupling augmented reality displays. *Opt Express*. 2017;25(22):27008–27014. <https://doi.org/10.1364/OE.25.027008>
- Xiang X, Escuti M. Numerical analysis of Bragg regime polarization gratings by rigorous coupled-wave analysis. *Proc SPIE*, 10127. 2017;101270D. <https://doi.org/10.1117/1.2258529>
- Lee YH et al. Compact see-through near-eye display with depth adaption. *J Soc Inf Display*. 2018;26(2):64–70. <https://doi.org/10.1002/jsid.635>
- Levola T et al., “Display system” U.S. Patent 9,372,347 B1 (2016)
- Lee HY et al., “Waveguide display with a small form factor, a large field of view, and a large eyebox” U.S. Patent 10,185,454, B2 (2019)
- Zhan T et al. Fabrication of Pancharatnam–Berry phase optical elements with highly stable polarization holography. *Opt*



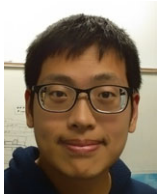
Express. 2019;27(3):2632–2642. <https://doi.org/10.1364/OE.27.002632>

28. Wu ST. Birefringence dispersions of liquid crystals. *Phys Rev A*. 1986;33(2):1270–1274. <https://doi.org/10.1103/PhysRevA.33.1270>
29. Parri OL, et al., "Birefringent layer with negative optical dispersion," U.S. Patent 8,119,026 B2 (2012).

## AUTHOR BIOGRAPHIES



**Tao Zhan** received his BS degree in Physics from Nanjing University in 2016 and is currently working toward a PhD degree from the College of Optics and Photonics, University of Central Florida. His current research interests include AR/VR system designs, liquid crystal optical elements, and computational diffractive optics.



**Yun-Han Lee** received the BS degree in Physics from National Central University in 2011 and MS degree in Physics from National Taiwan University in 2013 and is currently working toward the PhD degree from the College of Optics and Photonics, University of Central Florida, Orlando. His current research interests include fast phase modulators and near-eye displays including augmented reality and virtual reality displays.



**Jianghao Xiong** received a BS degree in Physics from the University of Science and Technology of China in 2017 and is currently working toward a PhD degree from the College of Optics and Photonics University of Central Florida, Orlando. His current research interests include near-eye displays and novel liquid crystal display devices.

**Guanjun Tan** received a BS degree in Physics from University of Science and Technology of China in 2014 and is currently working toward the PhD degree at the College of Optics and Photonics, University of

Central Florida. His current research interests include head-mounted displays, organic LED displays, and novel liquid crystal display technologies.

**Kun Yin** received a BS degree in Opto-Electronics from Tianjin University of China in 2016 and is currently working toward a PhD degree from the College of Optics and Photonics, University of Central Florida, Orlando. Her current research interests include optical gratings and augmented reality and virtual reality displays.

**Jilin Yang** received a MS degree from College of Optical Sciences from the University of Arizona. He is currently an optical engineer at GoerTek Electronics, Santa Clara, California.

**Sheng Liu** received his PhD degree from College of Optical Sciences from the University of Arizona. He is currently the director of optical engineering at GoerTek Electronics, Santa Clara, California.



**Shin-Tson Wu** is Pegasus professor at College of Optics and Photonics, University of Central Florida. He is among the first six inductees of the Florida Inventors Hall of Fame (2014) and a Charter Fellow of the National Academy of Inventors (2012). He is a Fellow of the IEEE, OSA, SID, and SPIE and an honorary professor of National Chiao Tung University (2018) and of Nanjing University (2013). He is the recipient of 2014 OSA Esther Hoffman Beller Medal, 2011 SID Slottow-Owaki Prize, 2010 OSA Joseph Fraunhofer Award, 2008 SPIE G. G. Stokes Award, and 2008 SID Jan Rajchman Prize. Presently, he is serving as SID honors and awards committee chair.

**How to cite this article:** Zhan T, Lee Y-H, Xiong J, et al. High-efficiency switchable optical elements for advanced head-up displays. *J Soc Inf Display*. 2019;27:223–231. <https://doi.org/10.1002/jsid.767>